Antifungal and visible light driven photocatalytic degradation of Brilliant green dye by Ceria–Zirconia Nanocomposites

R. Tamilselvi[a], A. Thirumoorthi[b,*]
[a]*Research scholar, Centre for Research and Evaluation, Bharathiar University, Coimbatore – 641 046, Tamilnadu, India*
[b]*Associate Professor, Department of Chemistry, Government Arts College,Udumalpet – 642 126, Tamilnadu, India*

Green synthesis is a simple, eco-friendly and emerging approach of synthesizing Ceria-Zirconia nanocomposites (CZ NCs) and evaluates its performance for the photocatalytic treatment of industrial waste water. Ceria-Zirconia NCs were synthesized using leaf extracts of *Jatropha gossypiifolia L.* for the application towards photocatalytic degradation of Brilliant Green (BG) dye under visible light irradiation. The Ceria-Zirconia NCs were characterized by Fourier Transform Infrared (FT-IR) spectrometer, UV-Visible spectrophotometer, X-ray Diffraction (XRD), Scanning Electron Microscopy (SEM) equipped with Energy Dispersive X-ray Spectroscopy (EDX). FT-IR spectra indicate the presence of amino, carboxyl and hydroxyl functional groups on the crystal surface of the nanocomposites. In UV-Visible spectra, the nanocomposites exhibit the highest absorbance at about 252 and 340 nm. From XRD, the average crystallite size of the Ceria-Zirconia NCs were found to be 80.36nm, while SEM images showed the spherical clusters of agglomerated nanocomposites. The elemental composition and the purity of the nanocomposites were confirmed by Energy Dispersive X-ray Spectroscopy. The superior antifungal activity was investigated against with the fungal strains *Candida albicans, Aspergillus niger and penicillium.*

(Received February 7, 2024; Accepted May 15, 2024)

Keywords: Green synthesis, Ceria-zirconia NCs, Jatropha gossypiifolia leaf extract, Photocatalytic activity, Antifungal studies

1. Introduction

The green synthesis of nanoparticles/nanocomposites is having much attention in current research themes. The metal oxide nanoparticles synthesized by physical and chemical methods are very harmful to the environment, synthesized nanoparticles also generate a large amount of hazardous by-products and the materials used are highly expensive. Recently, non-toxic and eco-friendly chemicals have been used for the synthesis of nanomaterials [1-5]. Many plant extract mediated synthesis of metal oxide nanoparticles and mixed metal oxide nanocomposites, are more cost-effective, eco-friendly can easily be scaled up for large-scale commercial production and safe nature for the human therapeutic use also. The plant extract act as a capping as well as reducing agent to produce metal oxide nanoparticles in different size and morphology [6]. Biological approaches using plants extract for the synthesis of metal oxide nanoparticles are a safe alternative to chemical synthesis. Further, research on plant extract mediated green synthesis of nanoparticles also have higher, physico-chemical and optoelectronics properties that are great importance for application in the field of electronics, chemistry, agriculture and medicine [7]. Cerium oxide nanoparticles are rare earth oxides and are used in wide range of applications such as catalyst, solid oxide fuel cells, sensors, sunscreen cosmetics, therapeutics agents, antibacterial activities, antioxidant properties and anti-parasitic ointments [8-10]. Zirconium oxide nanoparticles has been studied for many applications such as fuel cells, catalysts, biosensors, oxygen sensors, toughened ceramics, optical dielectrics and antibacterial activities [11]. Past few years, cerium and zirconium

* Corresponding author: dramoorthiudt@gmail.com
https://doi.org/10.15251/JOBM.2024.162.99

mixed oxides have become a key factor in many heterogeneous catalysis applications. Moreover, the ceria-zirconia composites in nanoscale are key component of many catalysts and their supports, including photo catalysts due to their redox properties, oxygen storage capacity and high thermal stability [12-15].

Jatropha gossypiifolia is an Indian medicinal plant belonging to Euphorbiaceae family and contains approximately 175 species, cultivated throughout the tropical to temperate regions, have been used in various ailments like fever, stomach ache, tooth ache, eczema, cancer, tridosha, jaundice, anemia, carbuncles, dysentery, urinary discharges, abdominal complaints, fistula and disease of the heart [16, 17]. Pharmacological studies with different parts of *J. gossypiifolia* are shown to possess antibiotic, antioxidant, anti-inflammatory, antihypertensive, antimicrobial, anticholinesterase, hepatoprotective, insecticidal, pesticide properties and antidote for poisoning [18-20]. Ceria based nanoparticles have been synthesized from several plant extracts such as Aloe vera, Olea Europaea, Rubia cordifolia, Azadirachta indica, Lemon grass etc. [21-25].

Goutam et al. synthesized TiO_2 nanoparticles using leaf extracts of *J. Curcas* and reported that the green synthesized TiO_2 NPs showed the efficiency of 82.26% and 76.48% COD removal. The higher solar photocatalytic activity of green synthesized TiO_2 NPs can be attributed to the nano-size, pure crystalline anatase phase, large amount surface hydroxyl groups and higher surface area [26]. An aqueous leaf extract of *Jatropha curcas* was used for the synthesis of silver nanoparticles (Jc-AgNps) and evaluated for its antibacterial potential against food borne pathogens [27]. The synthesized Jc-AgNps showed the significant bactericidal activity against Gram-positive and Gram-negative bacteria and were highly effective against E.coli. The green synthesized CeO_2 Nps were effectively reduced the particle size to 3-5 nm and homogeneous particles distribution was observed and showed high photocatalytic acetaldehyde degradation in comparison to chemically synthesized CeO_2 which has particle size of 18-25 nm [28]. Zinc oxide nanoparticles were synthesized by using the leaf extract of *Jatropha gossypiifolia* for improving the photocatalytic and biological activity. The photo catalytic activities of ZnO Nps were investigated by the removal of methylene blue (MB) and malachite green (MG) organic dyes under UV light irradiation and found that the dye degradation efficiency of MB and MG were at 96% and 82% under UV light irradiation [29]. Ball-like Hexagonal Carbon-lignin/ Zinc oxide nanocomposites from castor leaves have been prepared [30] and found that they possessed highest photocatalytic performance on methylene blue at pH = 7.

The morphological effect of Zr-doped CeO_2 nanoparticles and the selective oxidation of styrene to styrene oxide using tert.butyl hydroperoxide as the oxidant have been studied by Renjia. It was found that Zr-doped CeO_2 nanoparticles exhibited the highest catalytic performance followed by nanoparticles and nanocubes. The enhanced catalytic activity of the Zr-doped CeO_2 nanoparticles was mainly attributed to the higher percentage of Ce^{3+} species and more oxygen vacancies [31]. The impact of zirconium doping on ceria NPs on optical, photocatalytic, dye degradation, antibacterial and antifungal activities have been investigated by Bakkiyaraj et al. [32]. The slight decrease in crystallite size with increasing zirconium content in the ceria lattice has been observed.

Premkumar et al. have been studied the synthesis of ceria–zirconia ($Ce_{0.5}Zr_{0.5}O_2$) mixed metal oxide (MMO) nanoparticles using *Meliadubia* leaf extract and investigated antimicrobial efficacy. The nanoparticles were screened for antibacterial and antifungal potential against the bacterial strains *Pseudomonas aeruginosa* and *Streptococcus mutans* and the fungal strain *Candida albicans*. The zirconia nanoparticles showed good antibacterial activity against gram-positive and gram-negative bacterial strains compared to the pristine ceria and MMO nanoparticles. In particular, the zirconia nanoparticles showed excellent antibacterial activity compared to the positive control Gentamicin. However, the ceria nanoparticles exhibited superior antifungal activity in comparison with the positive control employed in the experiment, Amphotericin B [33].

From the literature survey, it has been found that only few research articles have been published about photocatalytic and anti-fungal activities of ceria-zirconia mixed metal oxide nano composites and very few reports are available for the chemical synthesis of ceria-zirconia mixed metal oxide NCs. As per our knowledge from the literature, there is none of an article have been published still for the synthesis of ceria–zirconia mixed metal oxide nanocomposites by greener

route and hence the present study. In this paper, we have reported the synthesis, characterization of ceria-zirconia mixed metal oxide nanocomposites using *Jatropha gossypiifolia* leaf extract by greener method and the photocatalytic degradation of Brilliant green (BG) dye and the effect of pH on photocatalytic degradation have been studied. Also, the antifungal activities of CZ NCs against *Candida albicans, Aspergillus niger and penicillium* have been investigated.

2. Experimental

2.1. Chemicals and materials

Fresh leaves of *Jatropha gossypiifolia* were collected from Western ghats near Udumalpet, Tiruppur District, Tamilnadu, India. The plant material was authenticated by State Horticulture Experimental section, Tiruppur. Cerium nitrate and Zirconyl nitrate were chosen as the base materials. In the present work, required quantities of Cerium (III) nitrate [$Ce(NO_3)_3.6H_2O$] (Aldrich, AR grade, 99%) and Zirconyl (IV) nitrate [$ZrO(NO_3)_2.2H_2O$] (Aldrich, AR grade, 99%) were dissolved in double distilled water to get a homogeneous solution. The mixture is taken together in five Pyrex glass dishes in the molar ratios of 1:1, 0.8:0.2, 0.6:0.4, 0.4:0.6 and 0.2:0.8 and the samples obtained were labeled as CZJC-1, CZJC-2, CZJC-3, CZJC-4 and CZJC-5 respectively. The solid chemicals were used without any further purification. The double distilled water was used throughout the experimentation to make solution and washing purposes.

2.2. Preparation of plant extract

Fresh leaves of *Jatropha gossypiifolia* were used to make the extract. The leaves of 10g were taken, washed twice with double distilled water and cut into fine pieces. In order to prepare leaf extract, leaves were taken into 250 ml Erlenmeyer flask and 100ml of double distilled water was added and kept on a water bath for 40 minutes at 80^0C.Then the content is filtered using Whatman No: 1 filter paper and it was used for the synthesis of Ceria–Zirconia nanocomposites.

2.3. Synthesis of Ceria–Zirconia nanocomposites

Ceria–Zirconia nanocomposites were synthesized via a facile hydrothermal method at the molar ratio of Ce:Zr are 1:1, 0.8:0.2, 0.6:0.4, 0.4:0.6 and 0.2:0.8 respectively. Cerium nitrate [Ce $(NO_3)_3.6H_2O$] and Zirconyl(IV)nitrate [$ZrO(NO_3)_2.2H_2O$] were dissolved separately in double distilled water and mixed together in a Pyrex glass dish. 20 mL of *Jatropha gossypiifolia* leaf extract was added to the above mixture and stirred vigorously in a magnetic stirrer at 500 rpm to obtain a clear solution. The dish containing the reaction mixture was calcined at 500^oC for 2 hours to obtain pale yellow CZ nanocomposites and their compositions are given in Table. 1.

Table 1. Composition of synthesized Ceria–Zirconia nanocomposites.

Name of the samples	Formula of the nanocomposites	Mole ratio of Ce: Zr
CZJC–1	$CeZrO_2$ [CeO_2–ZrO_2]	1 : 1
CZJC–2	$Ce_{0.8}Zr_{0.2}O_2$	0.8 : 0.2
CZJC–3	$Ce_{0.6}Zr_{0.4}O_2$	0.6 : 0.4
CZJC–4	$Ce_{0.4}Zr_{0.6}O_2$	0.4 : 0.6
CZJC–5	$Ce_{0.2}Zr_{0.8}O_2$	0.2 : 0.8

2.4. Characterization techniques

UV–Visible absorption spectra of synthesized Ceria–Zirconia nanocomposites were recorded using double beam UV-Visible spectrophotometer (UV-V-670, JASCO, USA) equipped UV-Probe software. The FT–IR spectra of the samples were recorded from 4000–400 cm^{-1} on the IR Prestige-21 spectrometer, Shimadzu using KBr pellets. X-ray diffraction (XRD) measurements were carried out on a Shimadzu lab X-6000 diffractometer with Cu Kα radiation (λ=1.54A˚).

Scanning Electron Microscope was used to investigate the morphology of the nanocomposites with Energy Dispersive X-ray spectroscopy (SEM with EDX) carried out with Oxford Instruments, INCA PENTA FET X3.

2.5. Photocatalytic degradation

Brilliant green (BG) is a triphenylmethane dye of Malachite green series and is a basic cationic dye. BG dye was purchased from Merck (Germany) and was used without any further purification. One gram of BG dye was dissolved in a litre of double distilled water to get a dye solution with a concentration of 1000 mg/L as stock solution. The concentration of the other solutions tested in the current study can be made by dilution method. The pH of the solution was adjusted with 0.1M sodium hydroxide and 0.1 M hydrochloric acid solutions.

Brilliant green dye has been used for photocatalytic degradation under direct sun light irradiation for all the synthesized samples of CZJC–1, CZJC–2, CZJC–3, CZJC–4 and CZJC–5. In this case, several glass vessels containing 100 ml of dye solution (10 mgL^{-1} of dye) and different amounts of photo catalysts (10, 20 30, 40, 50 mg) were used to degrade the dye solution for 120 minutes.

At appropriate time intervals of 30, 60, 90, 120 minutes, about 5 mL of the samples were withdrawn from mixture by using a micropipette and centrifuged at 2000 rpm for 5 minutes. After centrifuged, the supernatants were analyzed for the determination of the final concentration of dye. The removal of BG dye was determined at 625 nm based on the absorption by using a UV–Visible spectrophotometer. The experiments at different pH values of 4 and 10 were also carried out, by adding 0.1M HCl and NaOH, to reveal the role of pH on photocatalytic activity of Ceria–Ziconia mixed metal oxide nanocomposites [34, 35].

The absorption spectra of dye are recorded in terms of change in intensity at λ_{max} of a dye. The percentage degradation of dye is calculated using the formula:

$$\text{Percentage of Degradation} = \left\{ \frac{C_0 - C_t}{C_0} \right\}$$

where, C_0 = Initial concentration of the dye solution

C_t = Final concentration of the dye solution.

3. Results and discussion

3.1. Ultraviolet-Visible spectra

UV–Vis. spectrum of pure cerium oxide gave a split absorption at 265 and 370 nm because of allowed $O^{2-} \rightarrow Ce^{4+}$ charge transfer transitions [36, 37] and pure ZrO_2 gave peaks maximum at 211 nm first and then at 295 nm [37]. UV–Vis. spectra of synthesized CZ nanocomposites gave peaks centered at about 310nm with high intensity indicates that the increase in the concentration of zirconium ions. The position of the absorption metal oxides moves towards red shift and hence the intensity of peak decreases with increasing the concentration of Zr as dopant. The absorption of mixed metal oxides is more intense than the pure Ceria as well as pure Zirconia.

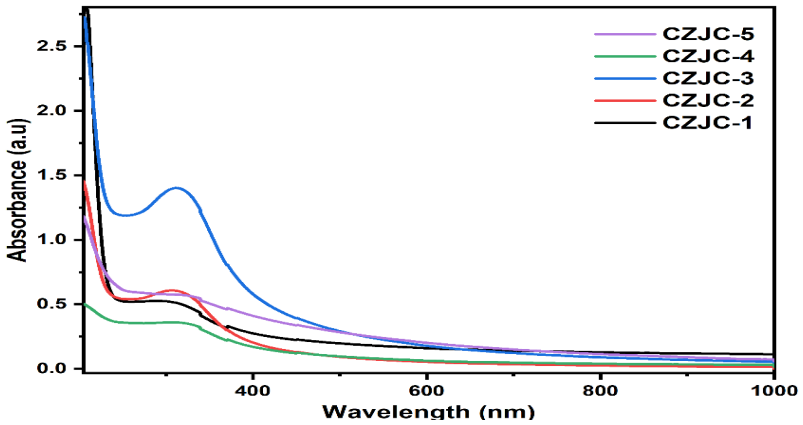

Fig. 1. UV-Vis. spectra of Ceria–Zirconia nanocomposites.

3.2. FT – IR spectra

FT–IR spectroscopy was used to identify the functional group present in the *Jatropha gossypiifolia* extract which acts as a capping/reducing agent in metal ions precursor. A strong peak at 3445 cm^{-1} is observed due to –OH group present in the leaf extract and a most intense band at 1367 cm^{-1} is also found because of methyl group symmetrical deformation in the compounds [39]. Another strong band at 1736 $cm^{-1}$is attributed to stretching vibrational frequency of C=O of anhydride and a peak at 1217.83 cm^{-1} is assigned to the stretching mode of C-N bond of amino functional groups [40]. A peak at 498 cm^{-1} is a characteristic peak of Ce–O stretching vibration which reveals fluorite like structure [41, 42] and an absorption peak at 400 cm^{-1} is assigned to Zr–O stretching vibration [43]. From the literature, it has been observed that pure CeO_2 gave a peak at 510 cm^{-1} and the introduction of Zr into Ceria crystal lattice matrix, the absorption shifts from 487 to 508 cm^{-1} which is in good agreement with the literature.

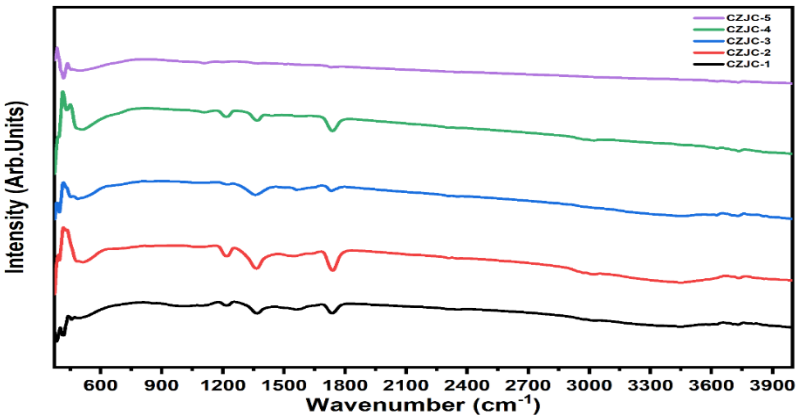

Fig. 2. FT-IR spectra of Ceria–Zirconia nanocomposites.

Table 2. FT–IR spectral data of synthesized Ceria- Zirconia nanocomposites.

CZJC-1		CZJC-2		CZJC-3		CZJC-4		CZJC-5	
Peak Position (cm^{-1})	**Assignment**	**Peak Position (cm^{-1})**	**Assignment**	**Peak Position (cm^{-1})**	**Assignment**	**Peak Position (cm^{-1})**	**Assignment**	**Peak Position (cm^{-1})**	**Assignment**
491.75	Ce-O	489.83	Ce-O	487.90	Ce-O	508.15	Ce-O	500.43	Ce-O
401.12	Zr-O	396.3	Zr-O	396.3	Zr-O	394.37	Zr-O	416.54	Zr-O
1217.83	C-N stretching	1217.83	C-N stretching	1217.82	C-N stretching	1216.86	C-N stretching	1254.46	C-N stretching
1559.17	Interaction between plant extract and metal oxides	1551.45	Interaction between plant extract and metal oxides	1560.13	Interaction between plant extract and metal oxides	1560.12	Interaction between plant extract and metal oxides	1560.12	Interaction between plant extract and metal oxides
1736.58	C=O stretching	1739.48	C=O stretching	1732.73	C=O stretching	1738.51	C=O stretching	1731.76	C=O stretching
3731.58	O-H stretching	3734.48	O-H stretching	3730.62	O-H stretching	3733.51	O-H stretching	3730.61	O-H stretching

3.3. X – ray diffraction studies

X–ray diffraction is a powerful, nondestructive system for characterizing crystalline materials. The peaks obtained for synthesized CZ nanocomposites are shown in Figure. 3 and the structural parameters are given in Table 3. The crystallographic parameters are in good agreement with JCPDS data card No. 28-0271 with cell dimension α=5.359 and wavelength λ=1.54056Å. The 2θ values are obtained at 28°, 33°,47°, 56°, 70° and 77°corresponds to (hkl) values of (111), (200), (220), (311), (400) and (331) planes respectively which clearly indicates the formation of Ceria–Zirconia nanocomposites having FCC structure [44]. Using the Debye –Scherrer equation, $D = (0.94\lambda)/\beta \cos\theta$, where λ is the radiation wavelength, β is the peak full width at half maximum (FWHM) and θ is the Bragg's angle, the average crystallite size 'D' was estimated. The unit cell parameters have been calculated using the most intense (111) plane of Ceria–Zirconia nanocomposites. From the table. 3, it has been observed that there is an increase in the lattice parameter from CZJC–1 to CZJC–3 and then decreases in CZJC–4 and CZJC–5 can be attributed to a shrinkage of the Ceria lattice due to the replacement of Ce^{4+} (0.97 A˚) ions with smaller cations, Zr^{4+} (0.84 A˚) in agreement with Vegard'slaw [45,46].The decrease in the lattice parameters can also be taken as an evidence for the formation of Ceria–Zirconia nanocomposites and the lattice parameter values obtained in the present study are in good agreement with the literatures [47,48].

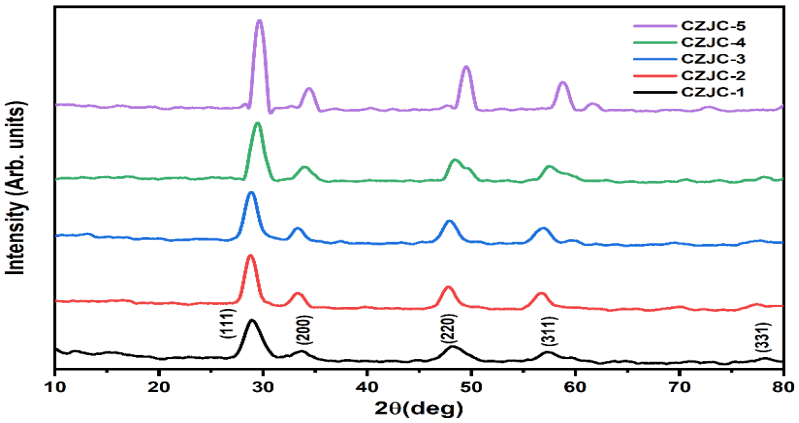

Fig. 3. XRD pattern of Ceria–Zirconia nanocomposites

Table 3. Structural parameters of Ceria–Zirconia nanocomposites.

Samples	Crystalline size (nm)	Lattice parameter (A°)	V $(A°)^3$
CZJC–1	46.65	5.3255	151.04
CZJC–2	81.50	5.4010	157.55
CZJC–3	67.59	5.4696	163.63
CZJC–4	62.41	5.2541	145.04
CZJC–5	161.11	5.2233	142.51

3.4. SEM analysis

Scanning Electron Microscopy has emerged as a valuable technique to investigate the structural and morphological characteristics of crystalline materials. High magnification SEM can reveal the surface nature, crystallite size and shape of crystalline materials. The morphology of the synthesized Ceria–Zirconia nanocomposites has been depicted in Figure 4. From the SEM images, it has been clearly observed that CZ NCs were agglomerated potentially due to their hygroscopic nature. Jibin.T.Philip et al. synthesized CeO_2 and Ce–Zr hybrid particles that results in the formation of enlarged and variation in particle size of significantly high [49].

SEM images (a, b, c, d, e) revealed that Ceria–Zirconia nanocomposites synthesized using *Jatropha gossypiifolia* leaf extract are polycrystalline with nano sized and granular in nature. These nanocomposites have particle size in the range from 46 to 161nm, in good agreement with particle size calculated. Introduction of Zr^{4+}ions into Ceria lattice enhanced the crystallite size from 46.65 to 161.11. At higher concentration of zirconium, the agglomerated spherical shape of nanocomposites has been formed [50].

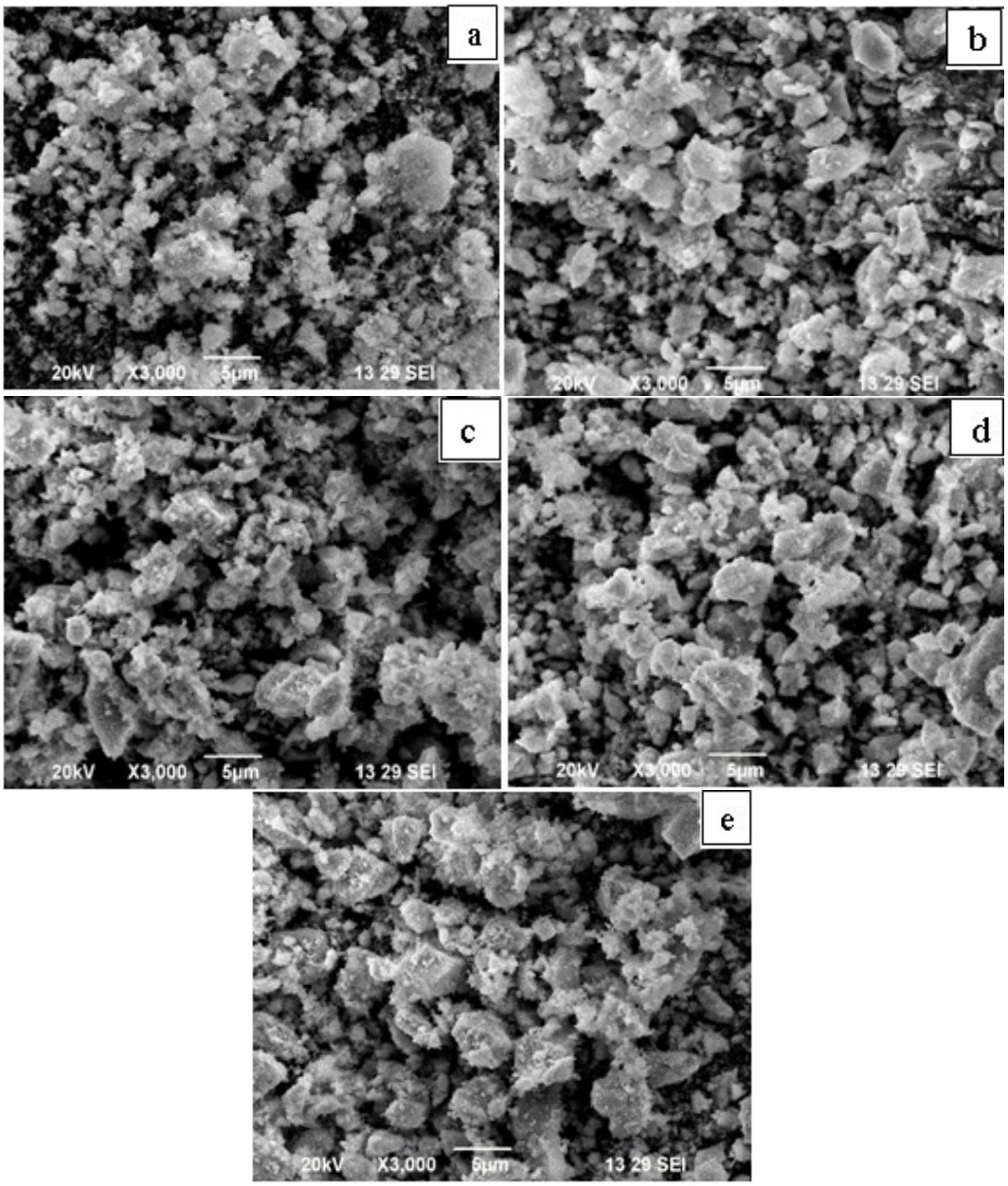

Fig. 4. SEM images of (a) CZJC–1 (b) CZJC–2 (c) CZJC–3 (d) CZJC–4 (e) CZJC–5.

3.5. EDX analysis

The Energy Dispersive X-ray (EDX) spectroscopic analysis is used to determine the elemental composition of synthesized Ceria–Zirconia nanocomposites which confirmed the presence of cerium, zirconium and oxygen in CZ NCs synthesized by greener way. Figure 5 showed the EDX spectra of the synthesized CZ NCs and Table.4 gives the weight percentage of each element present in the samples. EDX analysis confirmed the presence of Ce, Zr and O and revealed the formation of Ceria–Zirconia nanocomposites. Owing to the increase in concentration of Zr from 0.2 to 0.8 in Ceria lattice enhances the weight percentage in EDX spectra which confirmed the formation of Ceria–Zirconia nanocomposites with various molar ratio.

Table 4. Weight percentage of Ceria–Zirconia nanocomposites.

Samples	Composition	Ce	Zr	O
CZJC–1	$CeZrO_2$	70.52	5.99	23.49
CZJC–2	$Ce_{0.8}Zr_{0.2}O_2$	58.61	12.97	28.42
CZJC–3	$Ce_{0.6}Zr_{0.4}O_2$	56.17	23.60	20.23
CZJC–4	$Ce_{0.4}Zr_{0.6}O_2$	44.55	24.65	30.80
CZJC–5	$Ce_{0.2}Zr_{0.8}O_2$	32.92	37.96	29.13

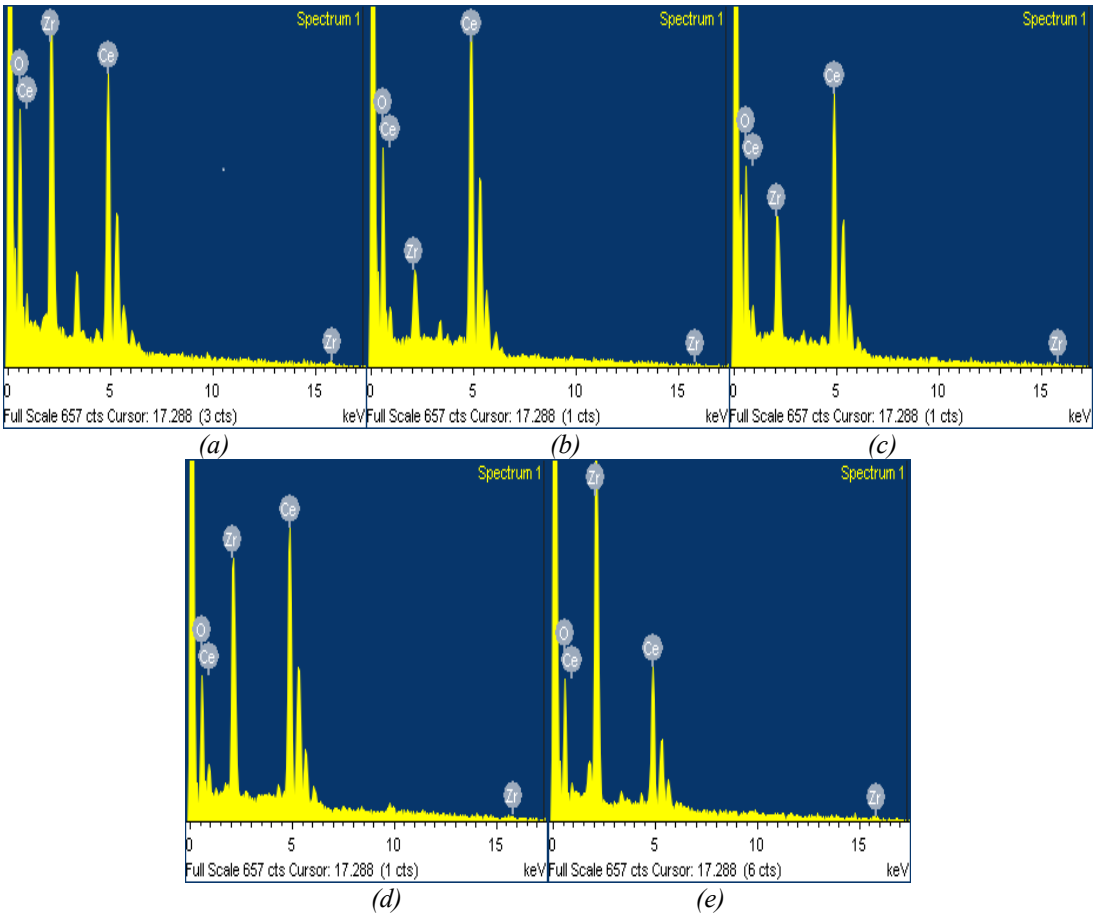

Fig. 5. EDX of (a) CZJC–1 (b) CZJC–2 (c) CZJC–3 (d) CZJC–4 (e) CZJC–5.

3.6. Photocatalytic measurements

Brilliant Green dye is one of the important dyes used in the paper printing and textile industries especially for dyeing wool and silk materials. Its effluents are also generated from rubber and plastic industries. BG dye is hazardous when contact with skin, eye and ingestion. It is toxic to the lungs, through inhalation and prolonged exposure to the substance can produce target-organ damage. During its decomposition it may generate carbon dioxide, sulphur oxides and nitrogen oxides. Therefore, it is important to remove Brilliant Green dye from industrial waste waters.

The influence of pH on the photocatalytic reaction is an important factor for the removal of dyes and other contaminants in waste waters. In the present study, the photocatalyst is highly dependent on pH as it affects the surface charge of the photocatalyst, degree of ionization and active sites of dye molecules. To investigate the effect of pH on dye removal, experiments were performed by adjusting the initial pH in the range of 4 to 10. Figure 6 shows the variation of pH

with percentage of dye removal observed during experiments. The figure indicates and observed that the pH of the medium increases during the reactive phase, then stabilizes at pH close to 8–10 depending on the initial pH. This increase in pH can be explained by the occurrence of water electrolysis resulting in hydrogen evolution and production of OH^- ions.

Figure 7, 8 and 9 depicts the variation of concentration of photocatalysts with their percentage degradation of Brilliant green dye removal at different pH of the medium. From the diagram, it is clearly indicates that at higher pH the percentage of removal of BG dye is more due to the facilitated formation of ·OH radicals.

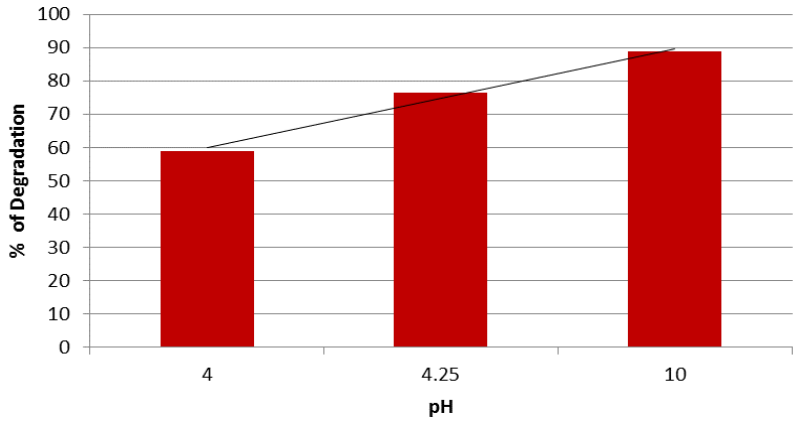

Fig. 6. Variation of pH with % of dye removal.

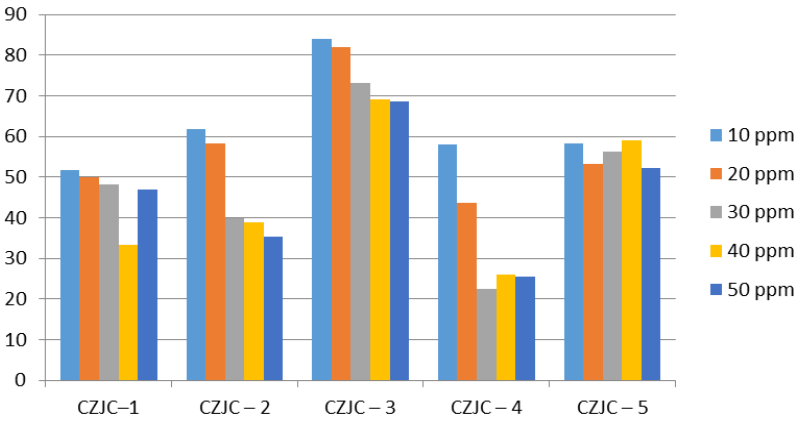

Fig. 7. Variation of % degradation of CZ NCs at natural pH.

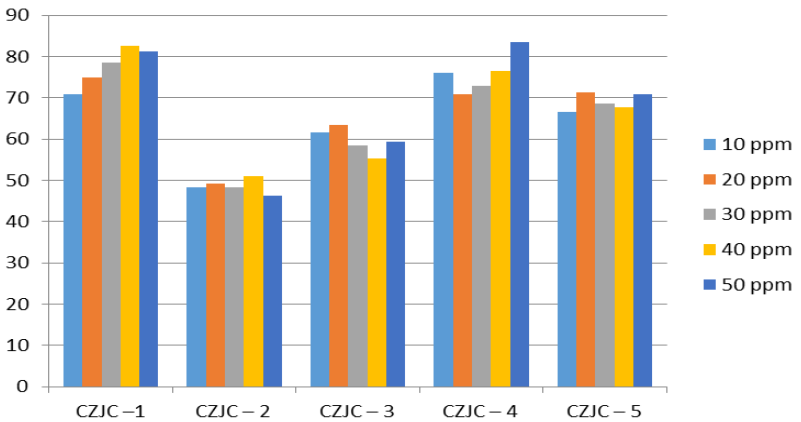

Fig. 8. Variation of % degradation of CZ NCs at pH = 4.

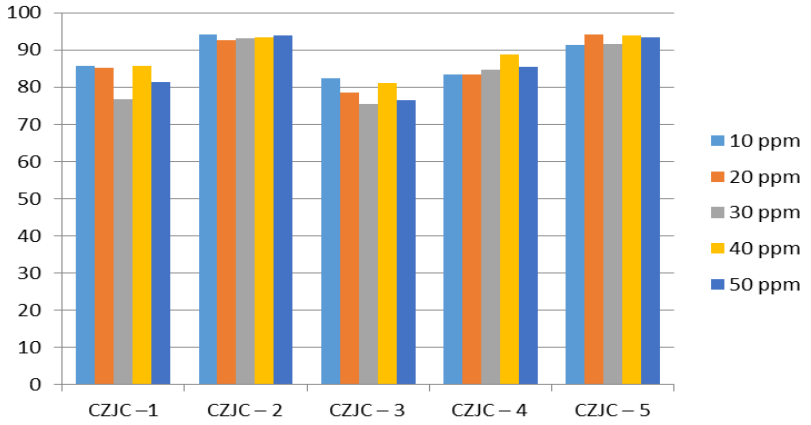

Fig. 9. Variation of % degradation of CZ NCs at pH = 10.

3.7. Mechanism of photocatalytic degradation

The general mechanism of photocatalytic degradation is given in Figure 10. In photo catalysis, when a material is irradiated with photons with energy equal to or higher than its band gap, electrons in the conduction band (CB) jumps to the valence band (VB) leaving positive holes and this stage is called reduction. As a result of reduction, the generated electrons and holes lead to the formation of reactive oxygen species (ROS) such as O_2 and ·OH (oxidation). The formation of ROS is the significant outcome of photo catalysis and can cause degradation of dye [51].

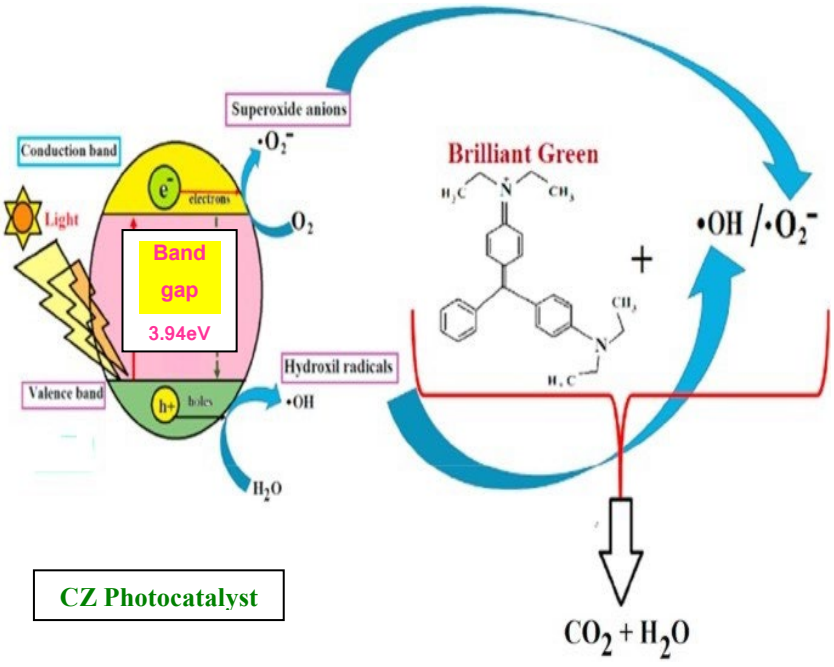

Fig. 10. General mechanism of Photo catalytic activity.

3.8. Antifungal studies

The antimicrobial behaviour of synthesized Ceria–Zirconia mixed metal oxide nanocomposites shown in Figure 11. The investigation of antifungal activities of CZ NCs concentration effects against *Candida albicans, Aspergillus niger and Penicillium* and exhibits the negative charge cell wall of the fungus has attracted by the positive charges ceria- zirconia mixed metal oxides. The equal molar ratio of Ceria- Zirconia mixed metal oxides has the better

interaction with the cell wall followed the electrostatic attraction and this could be the reason for disrupts the cell wall eventually cause fungus death.

The increase in concentration of Zirconium has effect in causing the improved antifungal activity as a result of increased ROS leading to destruction of the bacterial cell. On the other hand, the equal mole ratio of Cerium and Zirconium exposes the higher activity on the antifungal efficiency because of positive charge effect which creates the higher binding affinity with the fungal cell wall. The moderate antifungal activity of CZJC-3 was observed for *Penicillium* at concentration of 25 mg, 50 mg and100 mg correspond to 9, 13 and 17 zone of inhibition may be due to the sensitivity of nanoparticles associated with the different cell wall structures of fungi [52]. In the present study, we observed that CZJC – 1 shows higher zone of inhibition against *Candida albicans* while CZJC – 3 shows higher zone of inhibition against *Aspergillus niger* indicating that the difference in the crystallite nature of nanocomposites affecting the different cell wall structures of fungi under consideration.

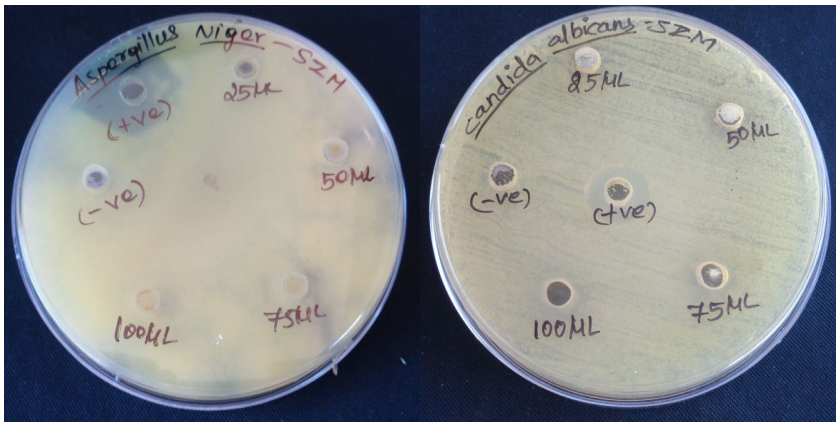

Fig. 11. Antifungal activity of synthesized Ceria-Zirconia mixed metal oxide nanocomposites.

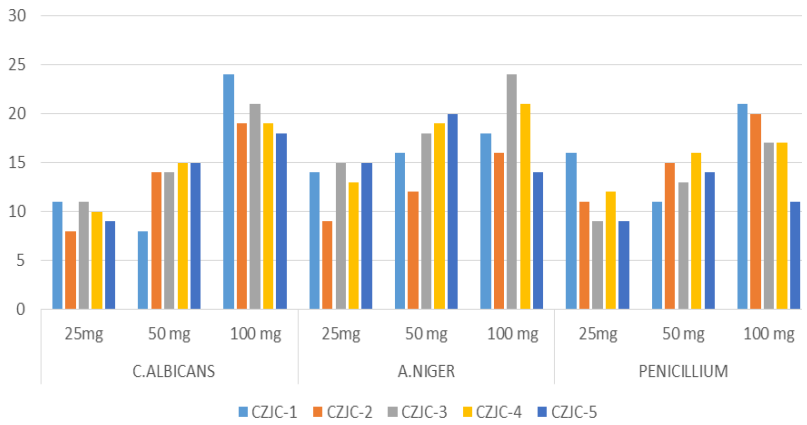

Fig. 12.Fungi – Zone inhibition of Ceria-Zirconia nanocomposites.

4. Conclusion

Ceria-Zirconia mixed metal oxide nanocomposites with varying mole ratios were produced successfully by green synthesis using *Jatropha gossypiifolia L.* leaf extract. UV-Visible spectra gives red shift and the intensity of the peak decreases with increase in the concentration of Zr as dopant. In FT-IR spectral analysis, Ce-O and Zr-O stretching frequencies confirmed the formation of CZ NCs and XRD shows the crystalline nature of the synthesized CZ NCs and the

size increases with increase in the concentration of Zr. SEM with EDX analysis confirmed the formation of agglomerated nanocomposites and the presence of Ce, Zr and Oxygen in the CZ NCs. The photocatalytic degradation of Brilliant green dye was observed more efficient in the basic medium (pH=10). The higher antifungal activities have been observed for CZJC−1 and CZJC−3 against *Candida albicans* and *Aspergillus niger* respectively whereas the other nanocomposites have moderate antifungal inhibition against chosen pathogens.

References

[1] R. R. Bhosale, A.S. Kulkarni, S.S. Gilda, N. H. Aloorkar, R. A. Osmani, B. R. Harkare, International Journal of Pharmaceutical Sciences and Nanotechnology.vol. **7,** No. 1, pp. 2328-2337, 2014; https://doi.org/10.37285/ijpsn.2014.7.1.3.

[2] X. Li, H. Xu, Z.-S. Chen, G. Chen, Journal of Nanomaterials, vol. **2011**, pp. 1–16, 2011; https://doi.org/10.1155/2011/270974.

[3] A.K. Khan, R. Rashid, G.Murtaza, A. Zahra, Journal of Pharmaceutical Research, vol. **13**, No. 7, pp. 1169-1177, 2014; https://doi.org/10.4314/tjpr. V13i7.23

[4] S. Gowri, R.R. Gandhi, M. Sundrarajan, Journal of Nanoelectronics Optoelectronics, vol.**8**, No. 3,pp. 240–249, 2013; http://dx.doi.org/10.1166/jno.2013.1466

[5] R. R. Gandhi, S. Senthil, R. Rajappan K. Ramesh, S. Gowri, J. Suresh J, M. Sundrarajan, Journal of Nanoengineering and Nonmanufacturing , vol. **5**, No. 1, pp.70-76, 2015; http://dx.doi.org/10.1166/jnan.2015.1224

[6] S. K. Kannan,and M. Sundrarajan, Bulletin of Material Science, vol. **38**, No.4, pp.945–950, 2015; http://dx.doi.org/10.1007/s12034-015-0927-7

[7] F. Caputo, M.De Nicola, A. Sienkiewicz, A. Giovanetti, I. Bejarano, S. Licoccia, E. Traversa L. Ghibelli, Journal of Nanoscale, vol.**7**, pp.15643 – 15656, 2015; http://dx.doi.org/10.1039/c5nr03767k

[8] T. Kubik, K. Bogunia-Kubik, M. Sugisaka, Current Pharmaceutical Biotechnology,Vol. 6, No.1, pp.17-33, 2005; https://doi.org/10.2174/1389201053167248;

[9] S. Das, J. M. Dowding, K. E. Klump, Nanomedicine, Vol. **8**, No.9, pp.1483–1508, 2013; http://dx.doi.org/10.2217/nnm.13.133

[10] C. Walkey, S. Das, S. Seal, Environmental Science, Vol. 2, No.1, pp.33-53,2015; https://doi.org/10.1039/C4EN00138A;

[11] D.G. Shchukin, R.A. Caruso, Journal of Advanced Functional Materials Vol. **13**, pp.789-794, 2003; http://dx.doi.org/10.1002/adfm.200304415

[12] Periyasamy, Kaliyappan, Aswathy, Venugopalan T, Ashok kumar, Venugopal, Manikandan, Marimuthu, Shukla, Rakesh,Tyagi, K. Avesh, Raja, Thirumalaiswamy RSC Advances, Vol. 5, pp.3619-3626, 2015; https://doi.org/10.1039/C4RA12355G

[13] M. Ozawa, Journal of Alloys Compounds, Vol. **275**, pp. 886–890. 1998; https://doi.org/10.1016/S0925- 8388(98)00477-0.

[14] S. Letichevsky, C.A. Tellez, R.R. de Avillez, M.I.P. da Silva, M.A. Fraga, L.G. Appel, Applied Catalyst B: Environmental, Vol.58, pp.203-210, 2005; https://doi.org/10.1016/j.apcatb.2004.10.014.

[15] X. Yang, X. Cheng, J. Ma, Y. Zou, W. Luo, Y. Deng, Small ,Vol.**15**, 1903058, 2019. https://doi.org/10.1002/smll.201903058

[16] R. P. Amarasingham, N. G. Bisset, A. H. Millard, M. C. Woods, Journal of Economic Botany, Vol. **18**, pp. 270-278, 1964; http://dx.doi.org/10.1007/BF02908122

[17] C. Chabra, F. C.Viso, E. N. Mshiu, Journal of Ethnopharmacology, Vol.11,pp.157-159, 1984 https://doi.org/10.1016/0378-8741(84)90037-0.

[18] A. S. Apu, F.Hossain,F. Rizwa, S. H. Bhuyan, M Matin, A.T.M, Jamaluddin, Journal of Basic Clinical Pharmacy, Vol.**4**, No. 1,pp. 20–24. 2013; http://dx.doi.org/10.4103/0976-0105.109404

[19] A.S. Apu, K.Ireen, S.H.HossanBhuyan, M.Matin, M. F.Hossain, and F.Rizwan, Journal of Medical Scence, Vol.**12**, No.8, pp.274-279. 2012; http://dx.doi.org/10.3923/jms.2012.274.279
[20] B. B.Panda, K. Gaur, M. L. Kori, L.K.Tyagi, R.K. Nema, C. S. Sharma and A.K. Jain, Global Journal of Pharmacology, Vol**3**, pp.1-5, 2009.
[21] D. Dutta D, R. Mukherjee, M. Patra M, Colloids Surface: B Biointerfaces., Vol.**147**, pp.45–53, 2016; http://dx.doi.org/10.1016/j. colsurfb.2016.07.045
[22] Q. Maqbool, M. Nazar, S.Naz S, International Journal of Nanomedicine, Vol.**11**,pp.5015–5025, 2016; http://dx.doi.org/10.2147/IJN. S11350
[23] N. Sisubalan, V. S.Ramkumar, A.Pugazhendhi, Environmental Science Pollution Research, Vol.25, No.11, pp.10482–10492, 2018; http://dx.doi.org/10.1007/s11356-017-0003-5
[24] J.K. Sharma, P. Srivastava, S. Ameen S, Material Research Bulletin, Vol.**91**, pp.98–107, 2017; http://dx.doi.org/10.1016/j.materresbull.2017.03.034
[25] S. Maensiri,S. Labuayai, PLaokul, Japanese journal of applied physics. Vol. **53**, No.6S, 06JG142014; http://dx.doi.org/10. 7567/JJAP.53.06JG14
[26] S.P. Goutam, G. Saxena, V. Singh, A. K. Yadav, R. N. Bharagava, and K. B. Thapa, Chemical Engineering Journal, Vol. **336**, pp.386–396; 2018; http://dx.doi.org/10.1016/j.cej.2017.12.029
[27] N. Chauhan, A.K. Tyagi, P. Kumar, A. Malik, Frontiers in Microbiology,Vol. **7**. 1748, 2016; http://dx.doi.org/10.3389/fmicb.2016.01748
[28] R. Magudieshwaran, J. Ishii, K. C. N. Raja, Materials Letters, vol. 239, pp. 40–44, 2019; https://doi.org/10.1016/j.matlet.2018.11.172
[29] B. R. Krishnan, M. Ramesh, and M. Selvakumar, Journal of Inorganic and Organometallic Polymers and Materials,Vol. **30**, pp.4441–4451, 2020; https://doi.org/10.1007/s10904-020-01576-9
[30] B. Ulum, S. Ilyas, and A.N. Fahri, Journal of Inorganic and Organometallic Polymers and Materials , Vol. **30**, 4905–4916, 2020; https://doi.org/10.1007/s10904-020-01631-5
[31] J. Ren, X. Liu, R. Gao and W-L. Dai, Journal of Energy Chemistry, Vol.26, No. 4, pp. 681-687, 2017.http://dx.doi.org/10.1016/j.jechem.2017.01.007
[32] R. Bakkiyaraj, M. Balakrishnan, G. Bharath, and N.Ponpandian, Journal of Alloys and Compounds, Vol. 724, pp. 555-564, 2017; http://dx.doi.org/10.1016/j.jallcom.2017.07.04
[33] NadarJebamerlin Selvaraj Janaki, D. S. Ivan Jebakumar, P. SumithrajPremkumar, Journal of Current Science and Technology, vol. 12, No.3, pp. 439-451
[34] Tayyebe Soltani, Mohammad H. Entezari, Journal of Molecular CatalysisA:Chemical, Vol. **377**,pp. 197 – 203, 2013; https://doi.org/10.1016/j.molcata.2013.05.004
[35] Ngoc Nhiem Dao, Minh Dai Luu, Ngoc Chuc Pham, Trung Dung Doan, Thi Ha Chi Nguyen, Quang Bac Nguyen, Thi Lim Duong, Advances in Natural Sciences:Nanoscience and Nanotechnology, Vol. **7,** 045003, 2016; http://dx.doi.org/10.1088/2043-6262/7/4/045003
[36] A. Bensalem, J. C. F. Muller, Bozon-Verduraz, Journal of the Chemical Soceity Faraday Tr7nsactions, Vol.88, pp. 153-154. 1992; https://doi.org/10.1039/FT9928800153
[37] R. Li , S. Yabe, M. Yamashita, S. Momose, S. Yoshida, S. Yin, T. Sato T, Material Chemistry Physics, Vol. **75**, No.1,pp.39-44, 2002; https://doi.org/10.1016/S0254-0584(02)00027-5
[38] S. Damyanova, B. Pawelec, K. Arishtirova, M.V.M. Huerta, J. L.G.Fierro, Applied Catalyst: A, Vol.**337**, No.1, pp. 86-96. 2008; https://doi.org/10.1016/j.apcata.2007.12.005
[39]U. Jeyapaul, M.J. Kala, A.J. Bosco, P. Piruthiviraj, M. Easuraja, Oriental Journal of Chemistry, Vol.**34**, pp. 783–790, 2018; http://dx.doi.org/10.13005/ojc/340223
[40] K. M. Kumar, B.K. Mandal, K. S. Kumar, P. S. Reddy, B. Sreedhar, SpectrochimicaActa Part A: Molecular and Biomolecular Spectroscopy, Vol. **102**, pp.128-133 2013; https://doi.org/10.1016/j.cej.2017.12.029
[41] S. Munusamy, K. Bhakyaraj, L. Vijayalakshmi, A. Stephen, V. Narayanan,International Journal of Innovative Research in Science and Engineering , Vol. **2**, No .1, pp.318-323, 2014.
[42] S. Jothi, N. Prithivikumaran, N. Jeyakumaran, International Journal of Chemical Technology Research, Vol. **6**, No.3 pp.1971-1973, 2014

[43] H. Zhang, Y. Liu, K. Zhu K, G. Siu G, Y. Xiong, C. Xiong, Journal of Physics: Condensed matter, Vol.11, 172035-2042.1999; https://doi.org/10.1088/0953-8984/11/8/016
[44] N. Pandiyan, B. Murugesan, J. Sonamuthu, S. Samayanan, S. Mahalingam S, Journal of Photochemistry and Photobiology B: Biology, vol. 178,pp.178:481-488, 2018 https://doi.org/10.1016/j.jphotobiol.2017.11.036
[45] M. Yashima, H. Arashi, M. Kakihana, and M. Yoshimura, Modeling and Local Structure of Solid Solutions. (1992) Journal of American Ceramic Society, vol.**75**, pp.1541–1549, 1992; https://doi.org/10.1111/j.1151-2916.1992.tb04222.x
[46] R. D. Shannon, Acta Crystallographica section A, Vol.32, pp.751-767,1976; https://doi.org/10.1107/S0567739476001551
[47] B. M. Weckhuysen, R. A. Schoonheydt, Catalyst Today, Vol. 49,pp.441- 451,1999 https://doi.org/10.1016/S0920-5861(98)00458-1
[48] X. Gao, I. E. Wachs, Journal of Physical Chemistry: B, Vol. **104**,pp. 1261–1268, 2000; https://doi.org/10.1021/jp992867t
[49] Jibin T Philip, Chacko Preno Koshy, M. D. Mathew, Materials Research Express, Vol. **6** , No.11, 2011; https://doi.org/10.1088/2053-1591/ab4fd5
[50] Mazhar Muhammad Ehsan, BakhtawarSamia, Rana Anwar Manzoor, Usmani Muhammad Nauman, AkhtarNaeem, Abbas Waseem, Materials Research Express Vol. **6**, No. 10, 105022, 2019; https://doi.org/10.1088/2053-1591/ab0f5f
[51] R.Tomar, A.A. Abdala, R.G. Chaudhary, N.B. Singh, Materials Today: Proceedings 2020; http://doi.org/10.1016/j.matpr.2020.04.144
[52] Ahmed A. Thamir, Najwa J. Jubier, Jafer F. Odah, Journal of Physics: Conference Series, 2114 012058, 2021; https://doi.org/10.1088/1742-6596/2114/1/012058